Protein Engineering, Design & Selection vol. 19 no. 7 pp. 299–307, 2006
Published online April 27, 2006 doi:10.1093/protein/gzl013

Engineered antibody–drug conjugates with defined sites and stoichiometries of drug attachment

Charlotte F. McDonagh[3], Eileen Turcott, Lori Westendorf, Jennifer B. Webster, Stephen C. Alley, Kristine Kim, Jamie Andreyka, Ivan Stone, Kevin J. Hamblett[1], Joseph A. Francisco[2] and Paul Carter[3]

Seattle Genetics, Inc., 21823 30th Drive SE, Bothell, WA 98021, USA

[1]Present address: Amgen, Inc., 1201 Amgen Court West, Seattle, WA 98119, USA

[2]Present address: Charles River Laboratories, 587 Dunn Circle, Sparks, NV 89431, USA

[3]To whom correspondence should be addressed.
E-mail: pcarter@seagen.com; cmcdonagh@seagen.com

The chimeric anti-CD30 IgG_1, cAC10, conjugated to eight equivalents of monomethyl auristatin E (MMAE) was previously shown to have potent antitumor activity against CD30-expressing tumors xenografts in mice. Moreover, the therapeutic index was increased by lowering the stoichiometry from 8 drugs/antibody down to 2 or 4. Limitations of such 'partially-loaded' conjugates are low yield (10–30%) as they are purified from mixtures with variable stoichiometry (0–8 drugs/antibody), and heterogeneity as the 2 or 4 drugs are distributed over eight possible cysteine conjugation sites. Here, the solvent-accessible cysteines that form the interchain disulfide bonds in cAC10 were replaced with serine, to reduce the eight potential conjugation sites down to 4 or 2. These Cys→Ser antibody variants were conjugated to MMAE in near quantitative yield (89–96%) with defined stoichiometries (2 or 4 drugs/antibody) and sites of drug attachment. The engineered antibody–drug conjugates have comparable antigen-binding affinities and *in vitro* cytotoxic activities with corresponding purified parental antibody–drug conjugates. Additionally, the engineered and parental antibody–drug conjugates have similar *in vivo* properties including antitumor activity, pharmacokinetics and maximum tolerated dose. Our strategy for generating antibody–drug conjugates with defined sites and stoichiometries of drug loading is potentially broadly applicable to other antibodies as it involves engineering of constant domains.

Keywords: auristatin/CD30/conjugate/engineered antibody

Introduction

Antibody conjugation to potent cytotoxic drugs is a promising way to enhance the antitumor activity of antibodies and reduce the systemic toxicity of drugs, as evidenced by numerous examples of preclinical efficacy and at least six antibody–drug conjugates currently in clinical development (Lambert, 2005; Wu and Senter, 2005). Clinical demonstration of the antibody–drug conjugate concept is provided by the approval of gemtuzumab ozogamicin (Mylotarg) for the treatment of acute myeloid leukemia (Bross *et al*., 2001). Gemtuzumab ozogamicin is a humanized anti-CD33 IgG_4 conjugated to calicheamicin, a highly cytotoxic natural product that induces double-stranded DNA cleavages (Hamann *et al*., 2002a,b). Other drugs that have been commonly conjugated to antibodies include auristatins and maytansinoids, which potently inhibit tubulin polymerization (Lambert, 2005; Wu and Senter, 2005).

Many different antibodies conjugated to auristatins have robust antitumor activity in mouse tumor xenograft studies including ones that target: CD30 (Doronina *et al*., 2003; Francisco *et al*., 2003), sialyl Lewis^y (Doronina *et al*., 2003), E selectin (Bhaskar *et al*., 2003), CD20 (Law *et al*., 2004), EphB2 (Mao *et al*., 2004), TMEFF2 (Afar *et al*., 2004) and CD70 (Law *et al*., 2006). For example, the chimeric anti-CD30 IgG_1, cAC10 (Wahl *et al*., 2002), was conjugated via its eight solvent-accessible cysteine residues to monomethyl auristatin E (MMAE) in near quantitative yield (Doronina *et al*., 2003). This homogeneous conjugate with 8 drugs/antibody was highly efficacious in SCID mouse xenograft models of anaplastic large cell lymphoma and Hodgkin's disease with a therapeutic index (curative dose/maximum tolerated dose) of 30–60 (Doronina *et al*., 2003; Francisco *et al*., 2003). A further 2- to 3-fold improvement in therapeutic index was achieved by reducing the drug stoichiometry from 8 drugs/antibody down to 2 or 4 drugs/antibody (Hamblett *et al*., 2004). A potential drawback of such 'partially-loaded' conjugates is heterogeneity in the stoichiometries and sites of drug attachment. For example, a conjugate with a mean stoichiometry of 4 drugs/antibody is a mixture with 0, 2, 4, 6 or 8 drugs/antibody (Hamblett *et al*., 2004; Sun *et al*., 2005). Conjugates with uniform stoichiometry of 2 or 4 drugs/antibody were obtained by purification of corresponding mixtures, albeit with substantial reduction in yield and remaining heterogeneity as the 2 or 4 drugs were distributed over eight possible conjugation sites.

Here, we have generated antibody–drug conjugates with defined sites and stoichiometries of drug loading as a possible way to enhance the clinical potential of this class of antibody therapeutics. The solvent-accessible cysteine residues in the antibody cAC10 were replaced with a homologous residue, serine, to generate variants with either two or four remaining accessible cysteines. The Cys→Ser variants were then used to generate homogeneous and precisely defined antibody–drug conjugates that were then compared extensively *in vitro* and *in vivo* with more heterogeneous antibody–drug conjugates derived from prior methods (Hamblett *et al*., 2004; Sun *et al*., 2005).

Materials and methods

Cells and reagents

The anaplastic large cell lymphoma line, Karpas-299 (CD30 positive), and the non-Hodgkin's lymphoma cell line, WSU (CD30-negative), were obtained from the Deutsche

Sammlung von Mikroorganism und Zellkulturen GmbH (Braunschweig, Germany). L540cy (CD30 positive), a derivative of the Hodgkin's disease cell line L540 adapted to xenograft growth, was developed by Dr Harald Stein (Institüt für Pathologie, University Veinikum Benjamin Franklin, Berlin, Germany). Cell lines were grown in RPMI-1640 media (Life Technologies, Gaithersburg, MD, USA) supplemented with 10% fetal bovine serum.

Mutagenesis and subcloning

The construction of cAC10, a chimeric form of the murine monoclonal antibody, AC10, has previously been described (Wahl *et al*., 2002). Mutants of cAC10 were generated in pBluescript vectors containing cDNAs for either cAC10 heavy (pBSSK-AC10H) or light (pBSSK-AC10L) chain using a Quikchange® Site-Directed Mutagenesis Kit (Stratagene, La Jolla, CA, USA) and pairs of complementary oligonucleotide primers. The plus strand primers for the heavy chain mutants were (mutated codons underlined):

C220S, 5′-GTTGAGCCCAAATCTTCTGACAAAACTCACACATGCCC-3′;

C226S, 5′-GACAAAACTCACACATCCCCACCGTGCCCAGC-3′;

C226S:C229S, 5′-GACAAAACTCACACATCCCCACCGTCCCCAGCACCTGAACTC-3′.

Sequential rounds of mutagenesis were performed to gene rate the C220S:C226S and the C220S:C226S:C229S mutants. Similarly, the plus strand primer for the light chain mutant was C218S, 5′-CTTCAACAGGGGAGAGTCTTAGACGCGTATTGG-3′ (mutated codon underlined). The cAC10 heavy chain variant cDNAs were excised from pBluescript using *Xho*I and *Xba*I and ligated into the mammalian expression vector pDEF38 (Running Deer and Allison, 2004) downstream of the CHEF EF-1α promoter. The cAC10 light chain variant cDNAs were excised from pBluescript with *Mlu*I and cloned into similarly cleaved pDEF38 downstream of the CHEF EF-1α promoter.

Antibody expression

The cAC10 variants were stably expressed in a CHO-DG44 cell line as previously described for the cAC10 parent antibody (Wahl *et al*., 2002). Briefly, 50 μg of each of the heavy and light chain expression constructs in vector pDEF38 were linearized with *Pvu*I and then coelectroporated into CHO-DG44 cells (Urlaub *et al*., 1986). Stable cell lines expressing the cAC10 variants (Table I) were selected in hypoxanthine and thymidine deficient EX-CELL™ 325 media (JRH Biosciences Inc., Lenexa, KS, USA). High titer clones identified by antigen-binding ELISA were recovered by limiting dilution cloning and cultured in spinner flasks (2.5 l) or WAVE bioreactors (5–10 l, WAVE Biotech LLC, Bridgewater, NJ, USA).

Antibody purification

The cAC10 parent and variant antibodies were purified by protein A followed by anion exchange chromatography using a FPLC (ÄKTAexplorer, GE Healthcare, Piscataway, NJ, USA). Briefly, the antibody-containing conditioned media were concentrated ~10-fold and buffer-exchanged into phosphate-buffered saline (PBS), pH 7.4 by tangential flow filtration (Millipore, Bedford, MA, USA). The concentrated samples were treated with 0.5% (v/v) Triton X-100 (Sigma, St Louis, MO, USA) with gentle stirring overnight at 4°C for endotoxin removal. Samples were loaded on to a protein A column (GE Healthcare) pre-equilibrated with PBS, pH 7.4. The column was washed with PBS, pH 7.4, 2–3 column volumes (CV) 0.5% v/v Triton X-100, 1 M NaCl in PBS, pH 7.4 then with PBS, pH 7.4 until a stable baseline was reached. Bound antibody was eluted from protein A with 30 mM sodium acetate, pH 3.6 and then dialyzed against 20 mM Tris–HCl, 10 mM NaCl, 1 mM EDTA, pH 8.0 (buffer A). The pooled antibody was then loaded on to Q sepharose (GE Healthcare) pre-equilibrated with buffer A and washed with 2–3 CV buffer A, 5–10 CV buffer A containing 0.5% (v/v) Triton X-100 and 5 CV buffer A. Antibodies were eluted from Q sepharose by either step or linear NaCl gradient from 10–500 mM NaCl in buffer A and dialyzed against PBS, pH 7.4. Purified antibodies were analyzed by SDS–PAGE and by TSK-Gel G3000SW HPLC size exclusion chromatography (Tosoh Bioscience, Montgomeryville, PA, USA).

Table I. Cys→Ser antibody variants

Variant name[a]	Location of Cys→Ser mutations[b]	Competition binding to Karpas-299 (IC_{50}, nM)[c]
C8	None (parent)	2.8 ± 0.1
C2v1	L214, H220, H226	2.2 ± 0.4
C2v2	H220, H226, H229	2.6 ± 0.4
C4v1	L214, H220	3.2 ± 0.4
C4v2	H226, H229	2.4 ± 0.1
C4v3	H220, H226	nd[d]

[a]cAC10 variants are identified by the number of solvent-accessible cysteine residues and, where necessary, a variant number. E.g. C2v1 denotes a cAC10 variant containing two solvent-accessible cysteine residues (Fig. 1).
[b]L, light chain; H, heavy chain; numbering scheme of Kabat *et al*. (1991).
[c]Mean (± SEM) for three or more independent experiments.
[d]nd, not determined. Antibody variant C4v3 was excluded from the remainder of this study as size exclusion chromatography suggested significant aggregation, and SDS–PAGE analysis was not consistent with the behavior anticipated for one interchain disulfide bond between heavy chains).

Antibody conjugation

Conjugation of cAC10 Cys→Ser antibody variants with either 2 (variants C2v1–E2 and C2v2–E2) or 4 (variants C4v1–E4 and C4v2–E4) equivalents of MMAE involved antibody reduction with a few (2.5–4) equivalents of tris(2-carboxyethyl)phosphine (Acros Organics, Geel, Belgium) and conjugation to maleimidocaproyl-valine-citrulline-*p*-aminobenzoyl-MMAE (vcMMAE) (Doronina *et al*., 2003) without removal of excess tris(2-carboxyethyl)phosphine. The extent of reduction was assessed prior to drug addition by purifying a small amount of the reduction reaction through a PD-10 column (GE Healthcare) and titrating the number of antibody-cysteine thiols with 5,5′-dithio-bis(2-nitrobenzoic acid) (Ellman, 1958). The reduced antibodies were reacted with vcMMAE for 60 min at 0°C and excess *N*-acetylcysteine (Acros Organics) then added to quench any unreacted vcMMAE. The reaction mixture was then diluted 5-fold with water and then loaded on to a hydroxyapatite column (Bio-Rad Laboratories, Hercules, CA, USA) equilibrated with 10 mM sodium phosphate pH 7.0, 10 mM NaCl. The column was washed with 5 CV of the same buffer and the conjugate eluted with 100 mM sodium phosphate, pH 7.0 and 10 mM NaCl. The

conjugates were concentrated and buffer-exchanged into PBS using Amicon Ultrafree centrifugal filter units (Millipore, Bedford, MA, USA).

The generation of cAC10 conjugates with a mean stoichiometry of 4 drugs/antibody, C8–E4 mixture (C8–E4M, range of 0–8 drugs/antibody), and 2 drugs/antibody, C8–E2 mixture (C8–E2M), have been described (Hamblett *et al*., 2004; Sun *et al*., 2005). C8–E2M was subjected to hydrophobic interaction chromatography to isolate conjugates loaded with a uniform stoichiometry of 4 drugs/antibody (C8–E4) and 2 drugs/antibody (C8–E2) as previously described (Hamblett *et al*., 2004).

Conjugate analysis

Antibody–drug conjugates were analyzed to determine the stoichiometry of drug loading using the molar extinction coefficients at wavelengths of 248 and 280 nm for the antibody (9.41×10^4 and 2.34×10^5 M^{-1} cm^{-1}, respectively) and drug (1.50×10^3 and 1.59×10^4 M^{-1} cm^{-1}, respectively), as previously described (Hamblett *et al*., 2004). The location of drug attachment to the antibody heavy and light chains was investigated by reverse phase HPLC using a PLRP-S column (Polymer Laboratories, Amherst, MA, USA; No. 1912-1802: 1000 Å, 8 μm, 2.1 × 150 mm) and solvents A [0.05% (v/v) trifluoroacetic acid in water] and B [0.04% (v/v) trifluroacetic acid in acetonitrile] at a flow rate of 1 ml/min at 80°C. The solvent conditions were as follows: isocratic 25% solvent B (3 min), linear gradient to 50% solvent B (25 min), linear gradient to 95% solvent B (2 min), linear gradient to 25% solvent B (1 min) and isocratic 25% solvent B (2 min). Prior to chromatography, antibody–drug conjugate samples (10–20 μl, 1 mg/ml) were reduced with 20 mM DTT at 37°C for 15 min to cleave the remaining interchain disulfide bonds.

Endotoxin measurement

Endotoxin levels in antibody and antibody–drug conjugate preparations were determined by quantitative kinetic or endpoint Limulus amebocyte lysate assay using a chromogenic substrate as described by the vendor (Cambrex, Walkersville, MD, USA). Briefly, the sample was mixed with the Limulus amebocyte lysate and substrate reagent, and the absorbance at 405 nm measured over time (WinKQCL, Cambrex) or after 15 min incubation for kinetic and endpoint assays, respectively. The sample-related inhibition or enhancement of the Limulus amebocyte lysate endotoxin reaction was also analyzed by spiking serial dilutions of the sample with constant endotoxin concentrations for the endotoxin measurement in the sample allowing simultaneous detection of quality and quantity of sample and sample-induced interference. The endotoxin level in samples was then determined from the endotoxin standard curve generated by each assay method, which is linear over a concentration range. All purified antibody and antibody–drug conjugates had $\leqslant$0.05 endotoxin units/mg protein, which is at least 5-fold below the endotoxin level judged acceptable for *in vivo* studies.

In vitro characterization of antibody variants and drug conjugates

Competition binding of the cAC10 antibody variants and their corresponding drug conjugates was undertaken to assess the impact of mutations and drug conjugation upon antigen binding. Briefly, cAC10 was first labeled with europium using a protocol from the vendor (Perkin-Elmer, Boston, MA, USA). CD30-positive Karpas-299 cells were then combined with serial dilutions of the cAC10 parent antibody, variants or corresponding antibody–drug conjugate in the presence of 1 μg/ml europium-labeled cAC10 in staining medium [50 mM Tris–HCl pH 8.0, 0.9% (w/v) NaCl, 0.5% (w/v) bovine serum albumin, 10 μM EDTA] for 30 min on ice then washed twice with ice-cold staining medium. Labeled cells were detected using a Fusion HT microplate reader (Perkin-Elmer). Data were baseline-corrected and reported as the percent of maximum fluorescence as calculated by the sample fluorescence divided by the fluorescence of cells stained with 1 μg/ml cAC10-europium alone.

Growth inhibition of CD30-positive Karpas-299 or L540cy cells or CD30-negative WSU non-Hodgkin's lymphoma cells treated with cAC10 Cys→Ser variant conjugates was determined by incubating conjugates with cells for 92 h followed by incubation with 50 μM resazurin for 4 h at 37°C. Dye reduction was measured using a Fusion HT microplate reader. Data were analyzed by a non-linear least squares fit to a four-parameter logistic equation using Prism v4.01 (GraphPad Software Inc, San Diego, CA, USA).

Pharmacokinetics

The pharmacokinetic properties of the antibody–drug conjugates (C2v1–E2, C2v2–E2, C8–E2, C4v1–E4, C4v2–E4, C8–E4 and C8–E4M) were evaluated in SCID mice. Groups of SCID mice (three mice/group) were administered with 10 mg/kg of test material based on the antibody component by tail vein injection. Blood samples were collected from each mouse via the saphenous vein at 1 h, 4 h, 1 day, 2 days, 4 days, 7 days, 15 days, 21 days, 28 days, 36 days, 42 days and 50 days post-injection and serum isolated. Serum concentrations of antibody–drug conjugates were measured by antigen-binding ELISA as described previously (Hamblett *et al*., 2004). The time course of serum concentrations for each animal was plotted and non-compartmental pharmacokinetic parameters were calculated with WinNonlin version 4.0.1 (Pharsight, Mountain View, CA, USA).

Xenograft models

A total of 5×10^6 Karpas-299 or L540cy cells were implanted into the right flank of C.B-17 SCID mice (Harlan, Indianapolis, IN, USA) to establish a subcutaneous disease model of anaplastic large cell lymphoma or Hodgkin's disease, respectively (Doronina *et al*., 2003; Francisco *et al*., 2003; Hamblett *et al*., 2004). Tumor volume was calculated using the formula, $(A \times B^2)/2$, where A and B are the largest and second largest perpendicular tumor dimensions, respectively. Tumor-bearing mice were randomly divided into groups of 8–10 animals when the mean tumor volume was 100 mm^3. Mice groups were treated with a single intravenous dose of an antibody–drug conjugate or alternatively left untreated. Conjugate doses of 6.0 and 12.0 mg/kg for the 2 drugs/antibody conjugates and 3.0 and 6.0 mg/kg for the 4 drugs/antibody conjugates were used for the L540cy xenograft studies. Conjugate doses of 0.5, 1.0 and 2.0 mg/kg for the 2 drugs/antibody conjugates and 0.5 and 1.0 mg/kg for the 4 drugs/antibody conjugates were used for the Karpas-299 xenograft models. Animals were euthanized when tumor volumes reached ~1000 mm^3.

Maximum tolerated dose

Groups of three rats (Sprague–Dawley) (Harlan) were injected with 40, 60 or 80 mg/kg of C2v1–E2, C2v2–E2 and C8–E2 and 20, 30 or 40 mg/kg of C4v1–E4, C4v2–E4, C8–E4 and C8–E4M via the tail vein to determine the single dose maximum tolerated dose. Rats were monitored daily for 14 days, and both weight and clinical observations were recorded. Rats that developed significant signs of distress were euthanized.

Results

Construction and expression of antibody Cys→Ser variants

The parent antibody for this study, cAC10, is a chimeric IgG_1 that binds to human CD30 (Wahl *et al*., 2002). Antibody cAC10, has four solvent-accessible interchain disulfide bonds that are readily reducible and conjugated in near quantitative yield to vcMMAE, a thiol-reactive auristatin derivative (Doronina *et al*., 2003). This homogeneous antibody–drug conjugate comprising the cAC10 parent antibody with 8 drugs/antibody is designated here as C8–E8 (Fig. 1A). The solvent-accessible cysteines in cAC10 were systematically replaced with a homologous residue, serine, to generate antibody variants with either four (C4v1, C4v2 and C4v3) or two (C2v1 and C2v2) remaining accessible cysteines (Table I and Fig. 1A). These engineered antibody variants were used to generate drug conjugates with defined stoichiometries and sites of drug attachment.

All antibody variants were stably expressed in CHO-DG44 cell lines at titers of 25–125 mg/l. The antibody variants were purified from 2.5 to 10 l cultures by protein A affinity and ion exchange chromatography (Table I) and then analyzed by size exclusion chromatography and SDS–PAGE. All variants electrophoresed under reducing conditions gave rise to two major bands consistent with the presence of heavy and light chains (data not shown). Under non-reducing conditions, all antibody variants except C4v3 gave electrophoretic patterns (Fig. 1B) consistent with their anticipated interchain disulfide bonding pattern (Fig. 1A). Antibody variant C4v3 was excluded from the remainder of this study on the basis of its unanticipated electrophoretic behavior and a size exclusion chromatography profile that suggested significant aggregation.

Preparation of antibody–drug conjugates

The cAC10 parent antibody (C8) was partially reduced to yield a mean of 2 or 4 free thiols/antibody and then reacted with vcMMAE. The corresponding conjugates, C8–E2M and C8–E4M, have a mean loading of 2 drugs/antibody and 4 drugs/antibody, respectively. C8–E2M and C8–E4M are mixtures of conjugates loaded with 0, 2, 4, 6 or 8 drugs/antibody (Hamblett *et al*., 2004; Sun *et al*., 2005). Conjugates with uniform stoichiometry of either 2 drugs/antibody (C8–E2) or 4 drugs/antibody (C8–E4) were purified from the C8–E2M mixture by hydrophobic interaction chromatography as previously described (Hamblett *et al*., 2004; Sun *et al*., 2005). MMAE conjugates of the Cys→Ser variants were generated by reduction of the corresponding antibodies followed by reaction with vcMMAE.

For each antibody–drug conjugate the observed drug loading stoichiometry by spectrophotometric (Hamblett *et al*., 2004) and reverse phase HPLC analyses (Sun *et al*., 2005) closely matched those expected (Table II). Peak area analysis following size exclusion chromatography suggests that all antibody–drug conjugates were >98% monomeric. The yield of the Cys→Ser variant conjugates (89–96%) was similar to the heterogeneous conjugate, C8–E4M (95%), but greatly improved over the more homogeneous conjugates C8–E4 (11%) and C8–E2 (27%) purified from C8–E2M (Table II). Somewhat higher

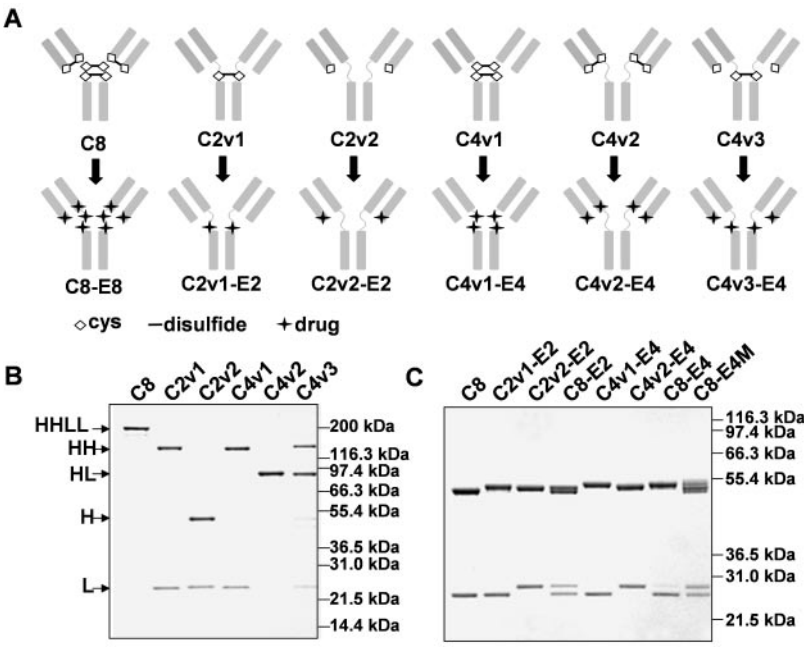

Fig. 1. Design and SDS–PAGE analysis of antibody Cys→Ser variants and corresponding drug conjugates. (**A**) Schematic representation of antibody variants and drug conjugates highlighting the location of solvent-accessible cysteines (diamonds), interchain disulfide bonds (–) and subsequently conjugated drugs (+). Antibodies and antibody–drug conjugates are identified by their variant name (see Table I), and loading stoichiometry with the drug, MMAE. For example, C8–E8 denotes the conjugate in which all eight solvent-accessible cysteine residues in the cAC10 parent antibody (C8) are conjugated to MMAE (E8). (**B**) SDS–PAGE analysis of antibody variants under non-reducing conditions. Arrows indicate the mobility of antibody heavy–light chain tetramer (HHLL), heavy chain dimer (HH), heavy–light chain dimer (HL), heavy chain (H) and light chain (L). (**C**) SDS–PAGE analysis of antibody–drug conjugates under reducing conditions.

Table II. *In vitro* characterization of antibody–drug conjugates

cAC10 drug conjugate[a]	Conjugate yield (%)[b]	Drugs/antibody: method 1, method 2[c]	Monomer (%)[d]	Competition binding to Karpas-299 (IC_{50}, nM)[e]	Karpas-299 cytotoxicity (IC_{50}, nM)[e]	L540cy cytotoxicity (IC_{50}, nM)[e]
C2v1–E2	92.7	2.0, 1.9	98.4	2.9 ± 0.3	0.26 ± 0.12	0.28 ± 0.03
C2v2–E2	88.9	2.1, 1.8	98.5	2.5 ± 0.1	0.46 ± 0.30	0.27 ± 0.02
C8–E2	27.4[f]	2.0, 2.0	99.7	2.8 ± 0.2	0.32 ± 0.21	0.28 ± 0.02
C4v1–E4	90.6	4.0, 3.8	99.2	3.2 ± 0.1	0.07 ± 0.02	0.13 ± 0.01
C4v2–E4	96.0	4.1, 3.8	99.0	2.8 ± 0.2	0.07 ± 0.02	0.12 ± 0.01
C8–E4	10.8[f]	4.0, 4.0	99.5	2.4 ± 0.3	0.07 ± 0.01	0.18 ± 0.04
C8–E4M	95	4.4, 4.4	98.8	3.0 ± 0.4	0.03 ± 0.01	0.07 ± 0.02

[a]Antibody–drug conjugates are identified by their cAC10 variant name (see Table I), loading level with the drug, MMAE, and whether the drug stoichiometry is uniform or variable (M). E.g. C8–E4M and C8–E2M denotes the parent antibody, cAC10, loaded with a mean stoichiometry of 4 drugs/antibody (range of 0–8 drugs/antibody) and 2 drugs/antibody (range of 0–8 drugs/antibody), respectively.
[b]Yield of conjugate obtained as a percentage of purified antibody. The free drug in all conjugate preparations was below the detection limit (<0.05%).
[c]Methods 1 and 2 refer to the ratio of absorbance at wavelengths of 248 and 280 nm (Hamblett *et al*., 2004) and reverse phase HPLC analysis under reducing conditions, respectively (Fig. 2).
[d]Estimated from the peak areas in size exclusion chromatography.
[e]Mean (± SEM) for three or more independent experiments.
[f]Percentage yield after hydrophobic interaction chromatography of C8–E2M based on the starting cAC10 protein. Yields of up to 30% C8–E4 have been achieved by using C8–E4M as a starting point for purification (S.Alley, unpublished data).

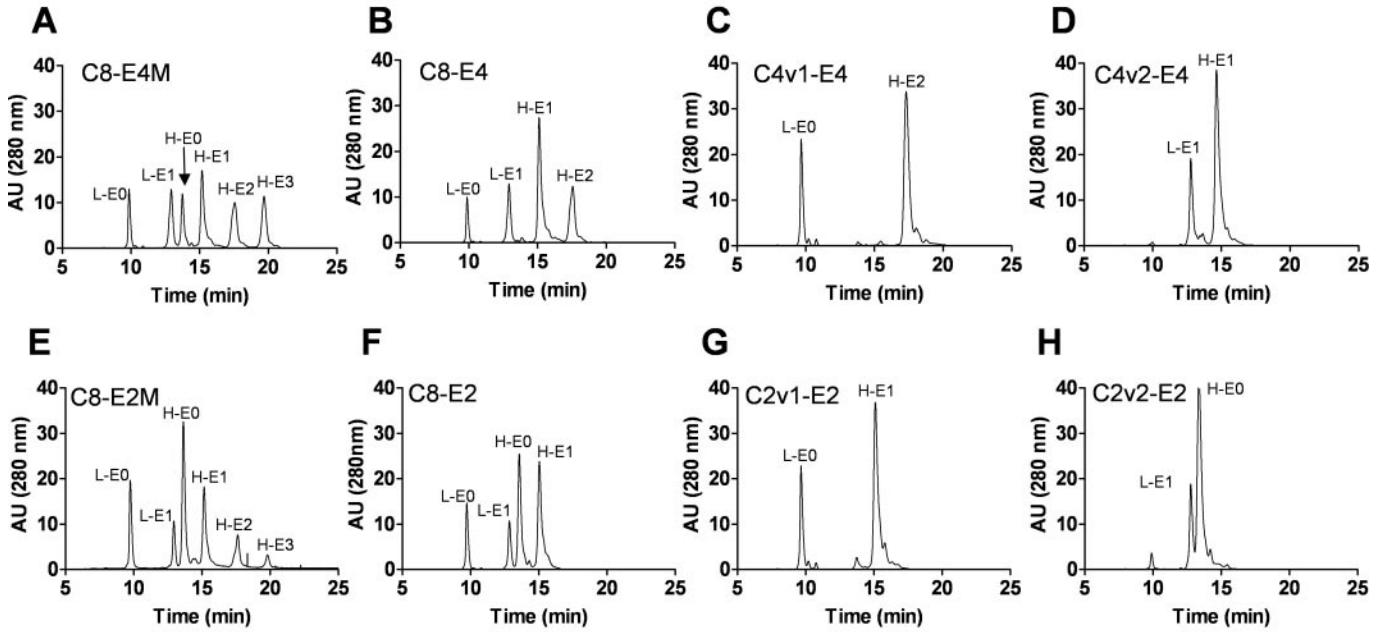

Fig. 2. Reverse phase HPLC analysis of antibody–drug conjugates under reducing conditions. (**A**) C8–E4M, (**B**) C8–E4, (**C**) C4v1–E4, (**D**) C4v2–E4, (**E**) C8–E2M, (**F**) C8–E2, (**G**) C2v1–E2 and (**H**) C2v2–E2 (see Table II). Peaks were identified by the ratio of their absorbance at wavelengths of 248 and 280 nm (see Materials and methods). L-E0 and L-E1 are used to denote light chains loaded with 0 or 1 equivalents of MMAE, respectively, whereas H-E0, H-E1, H-E2 and H-E3, indicate heavy chains loaded with 0, 1, 2 or 3 equivalents of MMAE, respectively.

yields (up to 30%) of C8–E4 have been achieved by using C8–E4M as a starting point for purification (S.Alley, unpublished data). SDS–PAGE analysis of the antibody–drug conjugates under reducing conditions fully resolves light chains loaded with 0 or 1 equivalents of MMAE (L-E0 and L-E1, respectively) and partially resolves heavy chains loaded with 0, 1, 2 or 3 equivalents of MMAE (H-E0, H-E1, H-E2 and H-E3, respectively), as shown previously (Doronina *et al*., 2003). For each Cys→Ser variant conjugate, a single light and heavy chain band with the anticipated mobility was observed (Fig. 1C). In contrast, more complex electrophoretic patterns were observed for C8–E2 and C8–E4M and to a lesser extent for C8–E4 (Fig. 1C).

Reverse phase HPLC under reducing conditions was used to further evaluate antibody–drug conjugate heterogeneity as this method can fully resolve all light and heavy chain species (Sun *et al*., 2005). C8–E4M (Fig. 2A) is the most heterogeneous conjugate containing all six possible species: L-E0, L-E1, H-E0, H-E1, H-E2 and H-E3. Purification of C8–E4M to generate C8–E4 reduces the heterogeneity down to four species: L-E0, L-E1, H-E1 and H-E2 (Fig. 2B). The homogeneity of cAC10 Cys→Ser variant conjugates is demonstrated by the presence of the anticipated single major light and heavy chain peaks: L-E0 plus H-E2, and L-E1 plus H-E1, for C4v1–E4 (Fig. 2C) and C4v2–E4 (Fig. 2D), respectively. Similarly for the 2 drugs/antibody conjugates C8–E2M (Fig. 2E) is the most heterogeneous containing all six possible species. Purification of C8–E2 (Fig. 2F) from C8-E2M reduces heterogeneity to L-E0, L-E1, H-E0 and H-E1. In contrast, C2v1–E2 (Fig. 2G) and C2v2–E2 (Fig. 2H) each gave rise to a pair of major peaks: L-E0 plus H-E1 and L-E1 plus H-E0, respectively.

In vitro characterization of antibody–drug conjugates

Competition binding experiments revealed that neither Cys→Ser mutations (Table I) nor vcMMAE conjugation (Table II) impaired antigen binding by the cAC10 antibody. Next the cytotoxicity of cAC10 Cys→Ser variant conjugates were assessed on CD30 positive (Karpas-299 and L540cy) and negative (WSU non-Hodgkin's lymphoma) cell lines. The C2v1–E2 and C2v2–E2 conjugates have very similar potency to C8–E2 on both CD30 positive cell lines (Table II). In addition, C4v1–E4, C4v2–E4, C8–E4M and C8–E4 conjugates displayed similar activity on both CD30 positive cell lines tested (Table II). Thus, defining the site and stoichiometry of drug attachment did not significantly impact the *in vitro* cytotoxic activity of the antibody–drug conjugates. Increasing the drug stoichiometry from 2 to 4 drugs/antibody increased the potency (reduced IC_{50} values), consistent with previous observations (Hamblett *et al*., 2004; Sun *et al*., 2005). CD30 negative WSU non-Hodgkin's lymphoma cells were insensitive to all cAC10 antibody–drug conjugates (data not shown).

Pharmacokinetics

SCID mice were dosed with various antibody–drug conjugates to determine how the sites and stoichiometries of drug loading would affect the pharmacokinetic properties. Immune deficient (SCID) rather than competent mice were chosen for consistency with the efficacy experiments (see below) and to avoid an antibody response to the antibody drug conjugates. SCID mice lack endogenous IgG and so administered IgG may potentially bind to endogenous Fc receptors on a variety of tissues and normal cells. Whilst this possibility was not explored in this study, it seems unlikely to have a major influence, since similar pharmacokinetic properties have been observed for chimeric antibodies in immune competent and Balb/c mice (Zuckier *et al*., 1994).

For cAC10 conjugated with MMAE, decreasing the loading from 8 drugs/antibody to 4 or 2 drugs/antibody was previously shown to decrease the clearance and increase the pharmacokinetic area-under-the-curve (Hamblett *et al*., 2004). We observed similar differences between the conjugates loaded with 2 drugs/antibody and 4 drugs/antibody. For example, the exposure of C2v1–E2, C2v2–E2 and C8–E2 was increased compared to C4v1–E4, C4v2–E4, C8–E4 and C8–E4M as determined by the area-under-the-curve (Table III). Also, clearance values for conjugates loaded with 2 drugs/antibody were lower than for those loaded with 4 drugs/antibody (Table III). Notably, there were only small differences in the pharmacokinetic area-under-the-curve or clearance values between C4v1–E4, C4v2–E4, C8–E4 and C8–E4M (Fig. 3A and Table III). Likewise, the pharmacokinetic parameters of C2v1–E2, C2v2–E2 and C8–E2 were similar (Fig. 3B and Table III).

Table III. Antibody–drug conjugate tolerability and pharmacokinetic parameters

cAC10 drug conjugate[a]	Maximum tolerated dose (mg/kg)[b]	Terminal half-life (days)	Area-under-the-curve (μg-day/ml)	Clearance (ml/day/kg)
C2v1–E2	40	13.1 ± 3.7	2210 ± 360	4.6 ± 0.8
C2v2–E2[c]	60	16.6	2460	4.4
C8–E2	40	15.9 ± 2.3	2790 ± 150	3.6 ± 0.2
C4v1–E4	20	17.4 ± 3.3	1800 ± 80	5.6 ± 0.2
C4v2–E4	<20	14.8 ± 1.3	1060 ± 220	9.7 ±2.2
C8–E4	20	11.8 ± 1.3	1700 ± 120	5.9 ± 0.4
C8–E4M	<20	13.1 ± 4.4	1420 ± 440	7.6 ± 2.7

[a]See Table II for antibody–drug conjugate nomenclature.
[b]The single dose maximum tolerated dose in Sprague–Dawley rats was defined as the highest dose that did not induce >20% weight loss or severe signs of distress.
[c]One mouse was found dead on Day 22 and eliminated from the pharmacokinetic analysis.

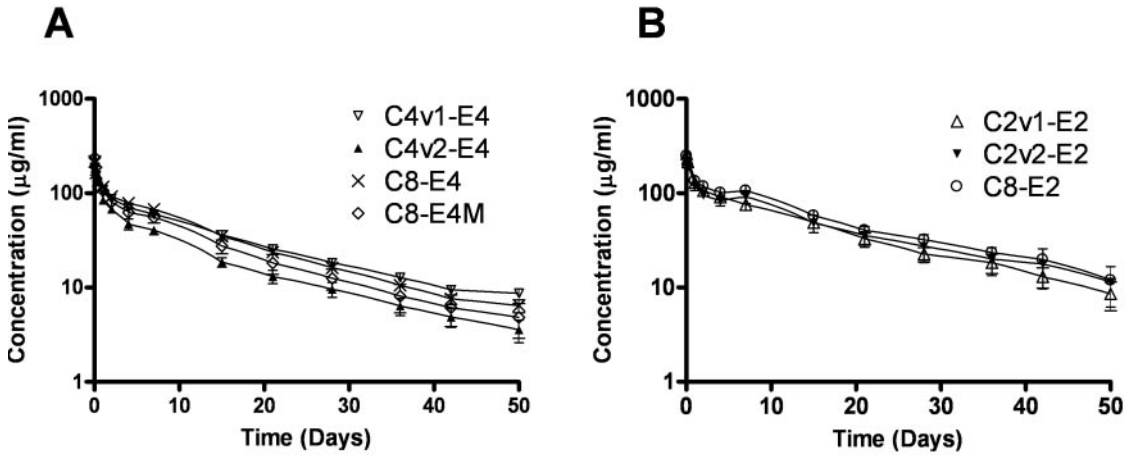

Fig. 3. Pharmacokinetics of antibody drug conjugates loaded with 4 drugs/antibody (**A**) and 2 drugs/antibody (**B**). SCID mice were treated with 10 mg/kg of conjugate and serum samples were collected and analyzed by ELISA to determine antibody–drug conjugate concentrations.

Antitumor activity of antibody Cys→Ser variant conjugates in vivo

The single dose efficacies of the cAC10 Cys→Ser variant drug conjugates were compared to conjugates of the parent antibody in established (~100 mm^3) subcutaneous xenograft models of Hodgkin's disease (L540cy) and anaplastic large cell lymphoma (Karpas-299) in SCID mice. A tumor that decreased in size such that it was impalpable was defined as a complete regression, whereas a complete regression that lasted beyond 100 days post-tumor implant was defined as a 'cure'. Treatment of L540cy xenograft models with C4v1–E4, C4v2–E4, C8–E4 and C8–E4M resulted in comparable responses with complete regressions being achieved at both 3.0 and 6.0 mg/kg for each antibody–drug conjugate (Fig. 4A and B). Treatment of Karpas-299 models with conjugates containing 4 drugs/antibody at doses of 0.5 and 1.0 mg/kg showed very similar and potent efficacy for all antibody–drug conjugates (data not shown). Responses of L540cy xenografts to treatment with C2v1–E2 and C2v2–E2 were comparable and complete regressions were induced at both 6.0 and 12.0 mg/kg doses (Fig. 4C and D). C8–E2 was slightly more potent than C2v1–E2 and C2v2–E2 with cures achieved at both dose levels (Fig. 4C and D). Karpas-299 xenograft models treated with single doses of the conjugates containing 2 drugs/antibody showed similar response trends with 3 of the 10 animals achieving complete regressions for C2v1–E2 and C2v2–E2 and 8 of 10 complete regressions for C8–E2 at a 1.0 mg/kg dose (data not shown).

Maximum tolerated dose

The maximum tolerated dose was defined as the highest dose that did not induce >20% weight loss or severe signs of distress. Previously, the single dose maximum tolerated dose of C8–E2 in BALB/c mice was shown to be >250 mg/kg (Hamblett *et al*., 2004; Sun *et al*., 2005)—the highest dose that could be readily tested. Sprague–Dawley rats were chosen here to assess the single dose tolerability of each antibody–drug conjugate. These rats are more sensitive than mice to the anti-CD30 MMAE conjugates and so permit more precise determination of the maximum tolerated dose for conjugates with 2 drugs/antibody. The cAC10 antibody (Wahl *et al*., 2002) binds to human CD30 but does not cross-react with the corresponding antigen from rats or mice. Thus, antigen-independent but not antigen-dependent toxicities of cAC10 drug conjugates can be explored in these species.

All conjugates loaded with 2 drugs/antibody were tolerated by rats at higher doses than those with 4 drugs/antibody, consistent with previous studies of C8–E2 and C8–E4 tolerability in mice (Hamblett *et al*., 2004; Sun *et al*., 2005). Minor differences in tolerability were observed between C2v1–E2,

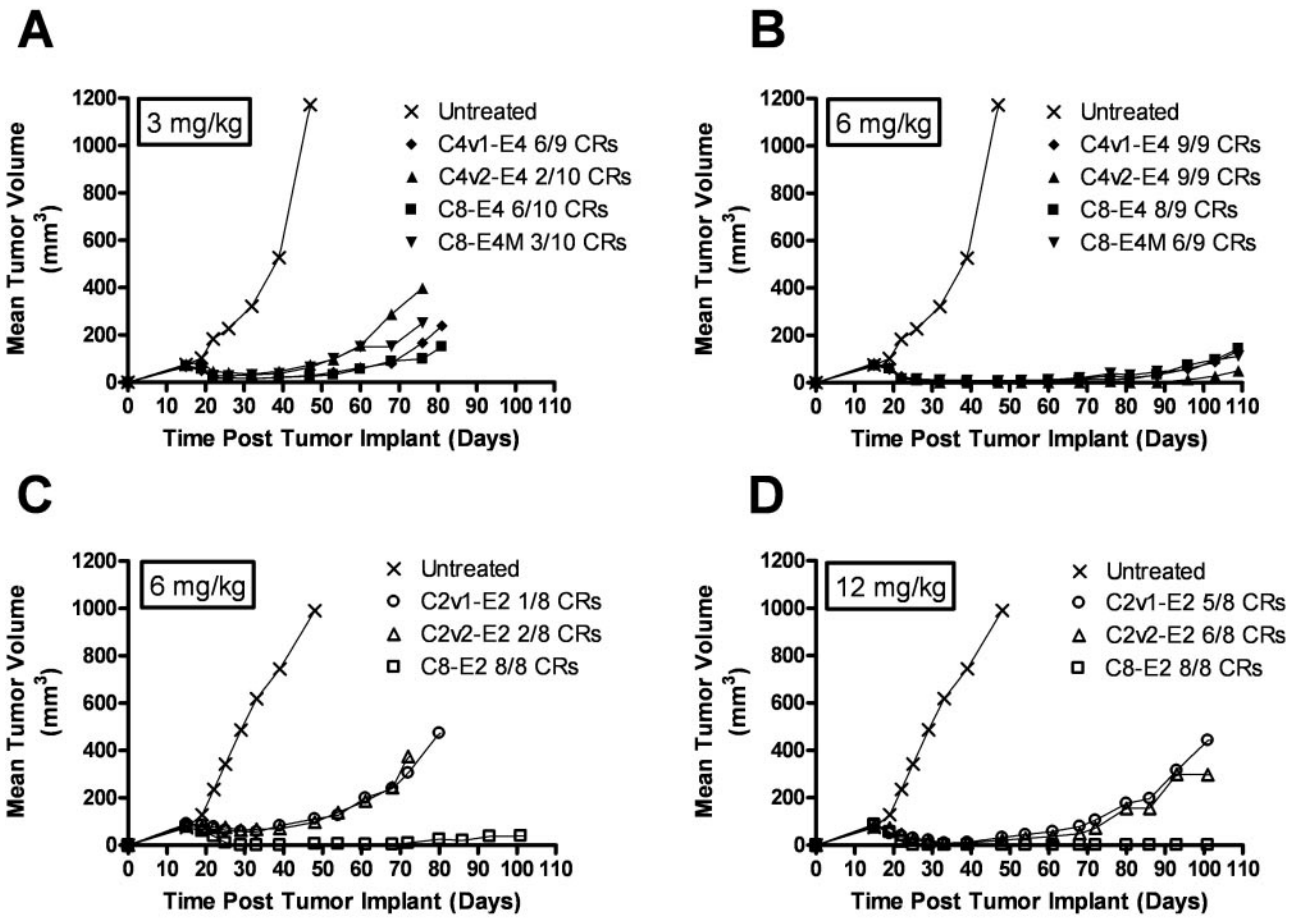

Fig. 4. Single dose efficacy studies on SCID mice bearing L540cy subcutaneous xenografts. Mice were treated 12 days post-tumor implant with a single dose of C4v1–E4, C4v2–E4, C8–E4 and C8–E4M at 3.0 mg/kg (**A**) and 6.0 mg/kg (**B**). Mice were treated 12 days post-tumor implant with a single dose of C2v1–E2, C2v2–E2 and C8–E2 at 6.0 mg/kg (**C**) or 12.0 mg/kg (**D**).

C2v2–E2 and C8–E2, which were dosed at 40, 60 and 80 mg/kg. The 40 mg/kg dose of each conjugate was well tolerated whilst the 60 mg/kg dose was only well tolerated by rats treated with C2v2–E2 (Table III). The conjugates containing 4 drugs/antibody were each dosed at 20, 30 and 40 mg/kg. Again there were only small differences in tolerability between conjugates. Animals injected with the 20 mg/kg dose of C4v1–E4 and C8–E4 experienced no adverse effects while several animals in the groups treated with the 20 mg/kg doses of C4v2–E4 and C8–E4M showed signs of distress and one from each group was sacrificed on Day 9. Based on these data the maximum tolerated doses for C4v1–E4 and C8–E4 were determined to be 20 mg/kg while the maximum tolerated doses for C4v2–E4 and C8–E4M were determined to be <20 mg/kg (Table III). The slightly greater toxicity of C8–E4M than C8–E4 likely reflects, at least in part, the drug loading stoichiometry of 4.4 drugs/antibody and 4.0 drugs/antibody, respectively (Table II), and the known correlation of drug load and toxicity (Hamblett *et al*., 2004; Sun *et al*., 2005).

Discussion

Desirable attributes of antibody–drug conjugates for targeted therapy include linkers between antibody and drug that are stable in circulation but readily cleavable within the target cells to release active drug, high therapeutic index (curative dose/maximum tolerated dose) and homogeneous composition to facilitate drug development. An antibody–drug conjugate that comes close to meeting these criteria is the anti-CD30 antibody, cAC10, conjugated to auristatin E (MMAE) via the eight solvent-accessible cysteine residues through linkers that are cleavable by lysosomal proteases such as cathepsin B (Doronina *et al*., 2003; Francisco *et al*., 2003). Reduction in the drug stoichiometry from 8 drugs/antibody to 4 drugs/antibody or 2 drugs/antibody increased the therapeutic index by ⩾2-fold (Hamblett *et al*., 2004), albeit at the expense of reduced conjugate yield and increased heterogeneity (drug attachment site and stoichiometry).

Here, we have developed a protein engineering approach to generate homogeneous antibody–drug conjugates in high yield with precisely definable site and stoichiometry of drug attachment. The chosen strategy was to systemically replace the solvent-accessible cysteine residues with serines. These cysteine residues commonly form interchain disulfide bonds in IgG. Thus, success of our strategy relies upon biosynthetic assembly of IgG, as well as IgG structure and function under physiologic conditions, to be independent of the presence of disulfide bonds. Several prior observations suggest that this would likely be the case. First, biosynthetic assembly of antibody light and heavy chains relies upon non-covalent interactions and does not require a disulfide between light and heavy chains as shown by studies with engineered $F(ab')_2$ fragments (Rodrigues *et al*., 1993). Moreover, removing the interchain disulfide bond impacted neither the antigen binding affinity of a $F(ab')_2$ fragment nor its pharmacokinetic properties (Rodrigues *et al*., 1993). Second, removal of the inter-heavy chain disulfide bonds of an IgG_1 did not impact expression nor binding to antigen but did impair effector functions (Gillies and Wesolowski, 1990). Third, the pharmacokinetic properties of cAC10 IgG in mice were not significantly altered by reduction and carboxymethylation of all four interchain disulfide bonds (K.J.H. and J.A.F., unpublished data).

Antibody variants were generated with either six (data not shown), four or two remaining accessible cysteines that were then conjugated to the drug, MMAE, in near quantitative yield. These naturally occurring cysteine residues are distant from the antigen-binding variable domains and, as anticipated, neither their replacement with serines (Table I) nor drug conjugation (Table II) impacted antigen binding. Removal of two, three or all four of the antibody interchain disulfide bonds has minimal effect on the antibody multimerization state as judged by size exclusion chromatography. In addition, similar *in vitro* potencies of the various 2 drugs/antibody conjugates (C2v1–E2 and C2v2–E2 versus C8–E2) and 4 drugs/antibody conjugates (C4v1–E4 and C4v2–E4 versus C8–E4 and C8–E4M) (Table II) suggests that the engineered conjugates are stable at least over the 4 day time course of the assay.

The engineered conjugates with 4 drugs/antibody, C4v1–E4 and C4v2–E4, have comparable antitumor activity to the parental conjugates, C8–E4 and C8–E4M, in both L540cy (Fig. 4) and Karpas-299 (not shown) xenograft models and exhibit only small differences in tolerability by rats (Table III). The antitumor efficacy of the engineered conjugates with 2 drugs/antibody, C2v1–E2 and C2v2–E2, is slightly lower than for the parental conjugate, C8–E2, with only minor differences in tolerability by rats. Additionally, broadly similar pharmacokinetic properties were found for the conjugates with 2 drugs/antibody (C2v1–E2, C2v2–E2 and C8–E2) and amongst those with 4 drugs/antibody (C4v1–E4, C4v2–E4, C8–E4 and C8–E4M). Thus, efficacy, tolerability and pharmacokinetics of the engineered antibody–drug conjugates are impacted to only a minor extent by the chosen alternative sites of drug attachment. In contrast, reducing the stoichiometry of drug loading from 4 to 2 drugs/antibody reduces efficacy and increases tolerability with little net effect on the therapeutic index (Fig. 4 and Table III), consistent with previous observations (Hamblett *et al*., 2004). Surprisingly, the most heterogeneous conjugate C8–E4M (0–8 drugs/antibody with a mean of 4 drugs/antibody and variable sites of drug attachment) has similar *in vitro* and *in vivo* properties to the most homogenous conjugates, C4v1–E4 and C4v2–E4 (fixed stoichiometry of 4 drugs/antibody at defined sites). Thus, from this study in conjunction with prior work (Hamblett *et al*., 2004; Sun *et al*., 2005), the stoichiometry of drug attachment is a more critical determinant of antibody–drug conjugate potency and tolerability than is the site of drug attachment and conjugate homogeneity.

Comparable *in vitro* and *in vivo* properties notwithstanding, the engineered antibody–drug conjugates offer significant advantages for drug development over their purified parental counterparts (C8–E2 and C8–E4) in terms of improved yield (>90% versus ⩽30%) and reduced heterogeneity of sites of drug attachment. The engineered conjugates (C4v1–E4 and C4v2–E4) were produced in similar yield to the unpurified parental counterpart, C8–E4M) but are much more homogenous—a potentially significant advantage from a drug manufacturing standpoint. The precise definition of drug location and stoichiometry in the engineered antibody–drug conjugates described here contrasts with the heterogeneity of many antibody–drug conjugates [reviewed by Wu and Senter (2005)] including gemtuzumab ozogamicin (Mylotarg), the only FDA-approved antibody–drug conjugate. Gemtuzumab ozogamicin has a mean stoichiometry of 2–3 drugs/antibody attached via lysine residues with 50% of the antibody

being unconjugated (Hamann *et al*., 2002b) (gemtuzumab ozogamicin prescribing information).

Prior engineering of IgG for site-specific conjugation to cysteine residues involved the *addition* of cysteine residues rather than the *removal* of naturally occurring cysteines described here. For example, an extra cysteine residue was introduced at several different locations in the C_H1 domain of an IgG_4 (Lyons *et al*., 1990). Of these added non-hinge cysteines, the fully accessible ones were reversibly blocked, whereas less accessible cysteines were only partially (~50%) blocked and available thiols were site-specifically radiolabeled. Selective reduction of the blocked thiols proved difficult with only 50% thiol recovery being achieved without reduction of the hinge disulfide bonds. More recently, a cysteine residue was introduced at position 442 of the C_H3 domain of an IgG_4 (Stimmel *et al*., 2000). Again the cysteine residue was reversibly blocked but in this case mild and selective reduction conditions were devised and site-specific labeling achieved with a radionuclide chelator. The performance of such engineered conjugates *in vivo* has yet to be reported. Introducing cysteine residues into antibody domains can sometimes promote interchain and intermolecular disulfide bonds that are undesirable for antibody–drug conjugate applications. For example, installing an additional cysteine residue at position 444 in the C_H3 domain led to the formation of disulfide-linked IgG dimers with enhanced effector functions (Caron *et al*., 1992; Shopes, 1992), whereas a cysteine installed at position 119 in a C_H1 domain created a compact and tethered IgG with an additional disulfide bond between the two heavy chains (Shopes, 1993).

Reduced IgG interaction with Fcγ receptors may limit antibody uptake by non-target organs and improve tumor localization (Hutchins *et al*., 1995)—a potentially advantageous property for antibody–drug conjugate applications. Removal of the hinge region interchain disulfide bonds from an IgG_1 has been reported to greatly impair antibody-dependent cellular cytotoxicity, consistent with impaired Fc–Fcγ receptor interactions, and also reduce complement-dependent cytotoxicity (Gillies and Wesolowski, 1990). The parent antibody, cAC10, is inefficient in supporting antibody-dependent cellular cytotoxicity so we are currently exploring the impact of Cys→Ser mutations and drug conjugation on the effector functions of other antibodies.

Generation of C8–E2 or C8–E4 using partial reduction methods results in antibody–drug conjugates where the majority of MMAE is linked to cAC10 via the cysteines involved in forming the heavy–light chain disulfide bond and the hinge region interchain disulfides are left intact (Sun *et al*., 2005). While methods have been developed to produce C8–E2 and C8–E4 with the majority of MMAE linked to the hinge region (Sun *et al*., 2005), recombinant generation of C2v1–E2, C2v2–E2, C4v1–E4 and C4v2–E4 results in antibody–drug conjugates lacking all interchain disulfide bonds and thus reduces the potential for internalization by non-target tissues mediated by interactions with Fcγ receptors.

Much research has focused on optimizing drugs and linkers for antibody–drug conjugates (Lambert, 2005; Wu and Senter, 2005). Consideration of drug stoichiometry has also been shown to enhance the therapeutic window of cAC10vcMMAE antibody–drug conjugates (Hamblett *et al*., 2004; Sun *et al*., 2005). Here, we report that the antibody component of the antibody–drug conjugate can also be optimized to complement advances in drug and linker technologies and generate highly potent and homogeneous product candidates. The strategy developed here for generating antibody–drug conjugates with defined sites and stoichiometries of drug loading is potentially broadly applicable to other antibodies as it involves engineering of constant domains. Indeed, we have successfully used this approach to generate antibody–drug conjugates of a humanized anti-CD70 antibody (C.F.M., S.C.A. and P.C., unpublished data).

Acknowledgements

We thank Dr Peter Senter for helpful discussions and critical reading of the manuscript and Dr Carmel Lynch for her analysis of the pharmacokinetic data.

References

Afar,D.E. *et al*. (2004) *Mol. Cancer Ther*., **3**, 921–932.
Bhaskar,V. *et al*. (2003) *Cancer Res*., **63**, 6387–6394.
Bross,P.F. *et al*. (2001) *Clin. Cancer Res*., **7**, 1490–1496.
Caron,P.C., Laird,W., Co,M.S., Avdalovic,N.M., Queen,C. and Scheinberg,D.A. (1992) *J. Exp. Med*., **176**, 1191–1195.
Doronina,S.O. *et al*. (2003) *Nat. Biotechnol*., **21**, 778–784.
Ellman,G.L. (1958) *Arch. Biochem. Biophys*., **74**, 443–450.
Francisco,J.A. *et al*. (2003) *Blood*, **102**, 1458–1465.
Gillies,S.D. and Wesolowski,J.S. (1990) *Hum. Antibodies Hybridomas*, **1**, 47–54.
Hamann,P.R., Hinman,L.M., Beyer,C.F., Lindh,D., Upeslacis,J., Flowers,D.A. and Bernstein,I. (2002a) *Bioconjug. Chem*., **13**, 40–46.
Hamann,P.R. *et al*. (2002b) *Bioconjug. Chem*., **13**, 47–58.
Hamblett,K.J. *et al*. (2004) *Clin. Cancer Res*., **10**, 7063–7070.
Hutchins,J.T., Kull,F.C. Jr, Bynum,J., Knick,V.C., Thurmond,L.M. and Ray,P. (1995) *Proc. Natl Acad. Sci. USA*, **92**, 11980–11984.
Kabat,E.A., Wu,T.T., Perry,H.M., Gottesman,K.S. and Foeller,C. (1991) *Sequences of Proteins of Immunological Interest,* 5th edn. NIH, Bethesda, MD.
Lambert,J.M. (2005) *Curr. Opin. Pharmacol*., **5**, 543–549.
Law,C.-L. *et al*. (2004) *Clin Cancer Res*., **10**, 7842–7851.
Law,C.-L. *et al*. (2006) *Cancer Res*., **66**, 2328–2337.
Lyons,A., King,D.J., Owens,R.J., Yarranton,G.T., Millican,A., Whittle,N.R. and Adair,J.R. (1990) *Protein Eng*., **3**, 703–708.
Mao,W. *et al*. (2004) *Cancer Res*., **64**, 781–788.
Rodrigues,M.L., Snedecor,B., Chen,C., Wong,W.L., Garg,S., Blank,G.S., Maneval,D. and Carter,P. (1993) *J. Immunol*., **151**, 6954–6961.
Running Deer,J. and Allison,D.S. (2004) *Biotechnol. Prog*., **20**, 880–889.
Shopes,B. (1992) *J. Immunol*., **148**, 2918–2922.
Shopes,B. (1993) *Mol. Immunol*., **30**, 603–609.
Stimmel,J.B., Merrill,B.M., Kuyper,L.F., Moxham,C.P., Hutchins,J.T., Fling,M.E. and Kull,F.C. Jr (2000) *J. Biol. Chem*., **275**, 30445–30450.
Sun,M.M., Beam,K.S., Cerveny,C.G., Hamblett,K.J., Blackmore,R.S., Torgov,M.Y., Handley,F.G., Ihle,N.C., Senter,P.D. and Alley,S.C. (2005) *Bioconjug. Chem*., **16**, 1282–1290.
Urlaub,G., Mitchell,P.J., Kas,E., Chasin,L.A., Funanage,V.L., Myoda,T.T. and Hamlin,J. (1986) *Somat. Cell Mol. Genet*., **12**, 555–566.
Wahl,A.F., Klussman,K., Thompson,J.D., Chen,J.H., Francisco,L.V., Risdon,G., Chace,D.F., Siegall,C.B. and Francisco,J.A. (2002) *Cancer Res*., **62**, 3736–3742.
Wu,A.M. and Senter,P.D. (2005) *Nat. Biotechnol*., **23**, 1137–1146.
Zuckier,L.S., Georgescu,L., Chang,C.J., Scharff,M.D. and Morrison,S.L. (1994) *Cancer*, **73**, 794–799.

Received March 7, 2006; accepted March 14, 2006

Edited by E. Sally Ward